Description of nuclear structure effects in sub-barrier fusion by the interacting boson model

A. B. Balantekin and J. R. Bennett
Physics Department, University of Wisconsin, Madison, Wisconsin 53706

N. Takigawa
Department of Physics, Tohoku University, 980 Sendai, Japan

(Received 6 March 1991)

Nuclear structure effects are incorporated in the description of fusion reactions near the Coulomb barrier using the interacting boson model. Predictions of this model are compared with the geometrical model and with sub-barrier fusion and mean angular momentum data for the fusion of ^{16}O with the axially symmetric nuclei ^{154}Sm and ^{166}Er.

I. INTRODUCTION

It is by now well established that heavy-ion fusion cross sections below the Coulomb barrier are several orders of magnitude larger than one would expect from a one-dimensional barrier penetration picture [1]. After extensive theoretical investigations [2–6], it was concluded that this enhancement can be attributed to the coupling of the translational motion to an additional degree of freedom such as nuclear and Coulomb excitation, nucleon transfer, or neck formation. The resulting multidimensional barrier transmission problem can be treated in the coupled-channels formalism. Since numerical implementation of a coupled-channels calculation with many channels could be tedious, several approximate treatments were proposed. One such approximation is the adiabatic approximation, in which the internal degree of freedom is assumed to have a degenerate spectrum. Esbensen obtained an expression for the total cross section of vibrational nuclei which is an average over probabilities of penetration through one-dimensional barriers corresponding to given values of zero-point fluctuation amplitudes [2]. Chase *et al.* studied the scattering of spherical projectiles by deformed nuclei and found that one needs to average over planar orientations of the two nuclei with respect to the collision axis [7]. A geometric interpretation of the adiabatic model was given by Nagarajan *et al.* when the nuclei are either rotational or vibrational [8]. All those approximate treatments of coupled-channel effects in sub-barrier fusion, including a proper treatment of angular momentum coupling [9], conclude that the fusion cross section is given by the approximate adiabatic expression

$$\sigma_{\text{total}}=\sum_{i=1}^{M}\omega_i\sigma(i)\ , \tag{1}$$

where $\sigma(i)$ is the fusion cross section in the eigenchannel i where the real potential is $V_0(R)+\lambda_i f(R)$, and the weight factors ω_i satisfy the condition

$$\sum_{i=1}^{M}\omega_i=1\ . \tag{2}$$

In these equations M refers to the number of target states included in the coupled-channel calculations [8], $V_0(R)$ is the bare potential, and $\lambda_i f(R)$ is the coupling form factor multiplied by the eigenvalue in the channel i.

In the previous studies of sub-barrier fusion either the geometrical model of Bohr and Mottelson [10] or its simplifications were used to describe the nuclear structure effects. Especially in the path-integral formulation of the problem, an algebraic nuclear structure model would significantly simplify obtaining the solution in the adiabatic approximation. The interacting boson model of Arima and Iachello [11] is one such model which has been successfully employed to describe the low-lying collective states in medium heavy nuclei. In this paper the use of the interacting boson model to describe the nuclear structure effects in sub-barrier fusion is presented. Our analysis is similar in spirit to the work of Ginocchio *et al.* [12,13] where the interacting boson model (IBM) was used to treat the proton scattering off heavy nuclei in Glauber approximation.

In the next section we present the general formulation of the problem, briefly summarizing the results of Refs. [6] and [12] as well. In Sec. III we apply our formalism to the description of the sub-barrier fusion of axially symmetric nuclei, those represented by the SU(3) symmetry chain of IBM. Section IV includes a brief summary of our results and directions for future work. The relation between the "adiabatic" approximation of Sec. III and the rotating-frame (or no-Coriolis) approximation previously discussed in the literature [8,14] is elucidated in the Appendix.

II. FORMULATION OF THE PROBLEM

In the interacting boson model the low-lying collective quadrupole states of medium-heavy even-even nuclei are generated as states of a system of N bosons. These bosons are considered to approximate the $J^{\pi}=0^{+}$ and 2^{+} coherent pairs of valence nucleons. The monopole and quadrupole boson annihilation (creation) operators are denoted by s ($s^{\dagger}$) and d ($d^{\dagger}$), respectively. In this model, one generally assumes that the Hamiltonian H_{IBM}, which determines energy levels and wave functions, contains

one-boson terms, and boson-boson interaction terms.

We take the Hamiltonian describing the system of fusing nuclei to be

$$H=-\frac{\hbar^2}{2\mu}\nabla^2+V(R)+H_{\rm IBM}+H_{\rm int}\ , \tag{3}$$

where R is the radial distance between the nuclei and $H_{\rm IBM}$ is the Hamiltonian describing the collective states in either the target or the projectile. The Hamiltonian describing the coupling of translational motion to the excitation of nuclear levels is assumed to be of the form

$$H_{\rm int}=[g_0(R)P+g_2(R)T^{(2)}]\cdot Y^{(2)}(\hat{\mathbf{R}})\ , \tag{4}$$

where $g_0(R)$ and $g_2(R)$ are the coupling form factors to be specified, $\mathbf{R}$ is the vector joining the centers of mass of two colliding nuclei, $\hat{\mathbf{R}}$ is the angular part of this vector, and the multipole moment operators of the nucleus are expressed in terms of boson operators as [12]

$$T^{(2)}_m=[d^\dagger\times\tilde{d}]^{(2)}_m \tag{5a}$$

and

$$P_m=s^\dagger\tilde{d}_m=d^\dagger_m s,\quad m=2,1,0,-1,-2\ . \tag{5b}$$

Throughout this paper we use the notation of Ginocchio *et al.* [12] to emphasize similarities between our path-integral approach to fusion and the Glauber approximation approach to proton scattering.

In the following the IBM quantum numbers corresponding to a given symmetry chain are denoted by n and the total boson number is denoted by N. The amplitude for transition from an initial state characterized by R_i and n_i (which is taken to be the IBM ground state) to the final state characterized by R_f and n_f is [6]

$$K(R_f,n_f,T;R_i,n_i,0)=\int\mathcal{D}[R(t)]e^{(i/\hbar)S(R,T)}\mathcal{W}_{n_fn_i}[R(t),T]\ , \tag{6}$$

where $S(R,T)$ is the classical action for the translational motion and $\mathcal{W}_{n_fn_i}$ is the transition amplitude for the internal system

$$\mathcal{W}_{n_fn_i}[R(t),T]=\langle n_f|\hat{U}(R(t),T)|n_i\rangle\ , \tag{7a}$$

with $\hat{U}$ satisfying the differential equation

$$i\hbar\frac{\partial\hat{U}}{\partial t}=(H_{\rm IBM}+H_{\rm int})\hat{U} \tag{7b}$$

subject to the initial condition $\hat{U}(t=0)=1$. The elements of the S matrix are given by

$$S_{n_f,n_i}(E)=-\lim_{\substack{R_i\to\infty\\R_f\to-\infty}}\left[\frac{P_iP_f}{\mu^2}\right]^{1/2}\exp\left[\frac{i}{\hbar}(P_fR_f-P_iR_i)\right]\times\langle R_f,n_f|G^+(E)|R_i,n_i\rangle\ , \tag{8a}$$

where μ is the reduced mass of the system and the classical momenta are

$$P_i=P(R_i)\equiv\{2\mu[E-\epsilon_i-V(R_i)]\}^{1/2}\ , \tag{8b}$$

with ϵ_i and ϵ_f being the initial and final excitation energies of the internal system. The G-matrix elements can be written in terms of the transition amplitude given in Eq. (6) as

$$\langle R_f,n_f|G^+(E)|R_i,n_i\rangle=\int_0^\infty dT\,e^{+iET/\hbar}K(R_f,n_f,T;R_i,n_i,0)\ . \tag{9}$$

The quantity of interest in sub-barrier fusion is the inclusive transmission probability, $P(E)$, i.e., the total probability that the internal system emerges in any final state. We have

$$P(E)=\sum_{n_f=0}^{\infty}|S_{n_f,n_i}(E)|^2\ . \tag{10}$$

Substituting Eqs. (6) and (9) into Eq. (10) one obtains

$$P(E)=\lim_{\substack{R_i\to\infty\\R_f\to-\infty}}\left[\frac{P_iP_f}{\mu^2}\right]\int_0^\infty dT\,e^{(i/\hbar)ET}\int_0^\infty d\tilde{T}\,e^{-(i/\hbar)E\tilde{T}}\times\int\mathcal{D}[R(t)]\mathcal{D}[\tilde{R}(\tilde{t})]e^{(i/\hbar)[S(R,T)-S(\tilde{R},\tilde{T})]}\rho_M(\tilde{R}(\tilde{t}),\tilde{T};R(t),T)\ , \tag{11a}$$

where the two-time influence functional ρ_M is given as

$$\rho_M(\tilde{R}(\tilde{t}),\tilde{T};R(t),T)=\sum_{n_f}\mathcal{W}^*_{n_f,n_i}[\tilde{R}(\tilde{t});\tilde{T},0]\mathcal{W}_{n_f,n_i}[R(t);T,0]\ . \tag{11b}$$

In writing Eqs. (11a) and (11b), in the spirit of the adiabatic approximation we assumed that the energy dissipated to the internal system is small as compared to the total energy, and took P_f outside the summation over final states.

Since the interaction Hamiltonian, Eq. (4), was chosen to be a linear combination of the elements of the SU(6) algebra, if the excitation energies are neglected in Eq. (7b),

$$i\hbar\frac{\partial\hat{U}}{\partial t}=H_{\rm int}\hat{U}\ , \tag{7b'}$$

the evolution operator is an element of the SU(6) group. For the degenerate spectrum limit, using the complete-

ness of final states, the two-time influence functional can easily be shown to be the matrix element of an SU(6) rotation

$$\rho_M(\tilde{\mathbf{R}},\tilde{T};\mathbf{R},T)=\langle n_U^\dagger(\tilde{\mathbf{R}},\tilde{T})U(\mathbf{R},T)|n_i\rangle \ . \tag{12}$$

$H_{\rm int}$ of Eq. (4) can be written as the three-dimensional rotation of a reduced Hamiltonian by the angle $\hat{\mathbf{R}}$:

$$H_{\rm int}(\mathbf{R})=\mathcal{R}(\hat{\mathbf{R}})H_{\rm int}^{(0)}(R)\mathcal{R}^\dagger(\hat{\mathbf{R}}) \ , \tag{13a}$$

where the reduced Hamiltonian is [12,13]

$$H_{\rm int}^{(0)}(R)=\tilde{g}_0(R)P_0+\sum_{m=-2}^{2}\phi_m(R)d_m^\dagger d_m \ , \tag{13b}$$

with

$$\tilde{g}_0(R)=(\tfrac{5}{4}\pi)^{1/2}g_0(R) \ , \tag{14a}$$

$$\phi_0(R)=-(\tfrac{5}{56}\pi)^{1/2}g_2(R) \ , \tag{14b}$$

$$\phi_2(R)=(\tfrac{5}{14}\pi)^{1/2}g_2(R) \ , \tag{14c}$$

$$\phi_1(R)=-[\phi_0(R)+\phi_2(R)] \ , \tag{14d}$$

$$\phi_{-m}(R)=\phi_m(R) \ . \tag{14e}$$

Note that the reduced Hamiltonian depends only on the distance between the two nuclei, but not on the angle $\hat{\mathbf{R}}$. Consequently, the solution of Eq. (7b′) can be written as a product of a three-dimensional rotation (depending on the angle $\hat{\mathbf{R}}$) and a simpler SU(6) transformation (depending on the distance between the nuclei). The influence functional is calculated for a given path (not necessarily the classical one), hence the evolution operator depends on time through the time dependence of the path. In order to elucidate the adiabatic nature of our approximation we introduce the reduced evolution operator

$$U^{(0)}(\mathbf{R}(t))=\mathcal{R}^\dagger(\hat{\mathbf{R}}(t))U(\mathbf{R}(t)) \ . \tag{15}$$

Substituting Eqs. (13) and (15) into Eq. (7b′) one finds that the reduced evolution operator satisfies the equation

$$i\hbar\frac{\partial U^{(0)}}{\partial t}=\left[H^{(0)}(R(t))-i\hbar\mathcal{R}^\dagger(\hat{\mathbf{R}}(t))\frac{\partial\mathcal{R}(\hat{\mathbf{R}}(t))}{\partial t}\right]U^{(0)} \ . \tag{16}$$

In addition to ignoring the excitation energies, as a second approximation we assume that the time dependence of the angle $\hat{\mathbf{R}}$ is very slow and ignore the second term in the above equation. As we demonstrate in the Appendix, this approximation implies that only $M=0$ substates are excited in the target nucleus. A similar approximation is made when the internal motion is described by the geometrical model by neglecting the Coriolis term in the kinetic-energy operator [8,14–17]. This latter approximation represents fusion in the rotating frame, where the z axis points along the vector $\mathbf{R}$. It can be shown that in the rotating frame approximation only $M=0$ magnetic substates are present [16]. The physical consequences of the no-Coriolis (rotating-frame) approximation and the approximation made in neglecting the second term in Eq. (16) are the same since they both lead to a coupling form factor independent of L and I [8] and the excitation of only the $M=0$ substates. As a result, $U^{(0)}$ depends only on the distance between two nuclei, R, and the influence functional becomes the matrix element of the simpler SU(6) transformation depending only on R

$$\rho_M(\tilde{R},\tilde{T};R,T)=\langle n_i|U^{(0)\dagger}(\tilde{R},\tilde{T})U^{(0)}(R,T)|n_i\rangle \ . \tag{17}$$

It is now straightforward to calculate the influence functional for the various symmetry chains of the interacting boson model.

III. FUSION OF AXIALLY SYMMETRIC NUCLEI: THE SU(3) CHAIN

In this section we concentrate on the case where either the target or projectile nucleus is axially deformed and can be described by the SU(3) symmetry chain of IBM. If the interaction Hamiltonian of Eq. (13b) is assumed to be a generator of SU(3) group [18] then one can show that [12,13]

$$\phi_0(R)=\phi_1(R)=\phi_{-1}(R)=\frac{1}{2\sqrt{2}}\tilde{g}_0(R) \ , \tag{18a}$$

$$\phi_2(R)=\phi_{-2}(R)=-\frac{1}{\sqrt{2}}\tilde{g}_0(R) \ . \tag{18b}$$

Since the nuclei are initially in their ground states, to calculate the influence functional in Eq. (17) one needs to calculate the matrix element of the SU(6) rotation $U^{(0)\dagger}(\tilde{R},\tilde{T})U^{(0)}(R,T)$ for the ground state. Using the fact that the SU(3) ground-state band is generated from a boson condensate of intrinsic bosons [19], Ginocchio *et al.* calculated this matrix element [12,13]. Using their result the two-time influence functional can easily be written in terms of a hypergeometric function

$$\rho_M(\tilde{R},\tilde{T};R,T)=e^{-2iNB}F(-N,\tfrac{1}{2};\tfrac{3}{2};1-e^{6iB}) \ , \tag{19a}$$

where

$$B=\frac{1}{2\sqrt{2}}\left[\int_0^T\tilde{g}_0(R(t))dt-\int_0^{\tilde{T}}\tilde{g}_0(\tilde{R}(t))dt\right] \ . \tag{19b}$$

Since the interaction Hamiltonian, Eq. (4), was chosen to be proportional to the quadrupole transition operator, $\tilde{g}_0(R)$ scales as the matrix element of this operator. Hence we introduce the reduced form factor

$$\tilde{g}_0(R)=\frac{f(R)}{\langle 2_1^+||Q||0_1^+\rangle} \ . \tag{20}$$

The reduced form factor consists of nuclear and Coulomb parts:

$$f(R)=f_C(R)+f_n(R) \ , \tag{21a}$$

where the Coulomb part is [13,14]

$$f_C(R)=\begin{cases}\dfrac{3}{\sqrt{20\pi}}\beta Z_1Z_2e^2\dfrac{R_c^2}{R^3} & (R\geq R_c) \ , \qquad (21b)\\[2ex] \dfrac{3}{\sqrt{20\pi}}\beta Z_1Z_2e^2\dfrac{R^2}{R_c^3} & (R<R_c) \ , \qquad (21c)\end{cases}$$

and the nuclear part is [9]

$$f_n(R)=-\left[\frac{5}{4\pi}\right]^{1/2}\beta R_V\frac{dV_N}{dR}\ . \tag{21d}$$

In our calculations we take $R_C=R_V=1.2A^{1/3}$ fm. For the SU(3) symmetry chain the reduced matrix element is given by [18]

$$\langle 2_1^+||Q||0_2^+\rangle=\sqrt{2N(N+\tfrac{3}{2})}\ . \tag{22}$$

Substituting Eqs. (19) through (22) into Eq. (11a) after some steps we obtain the total fusion cross section to be

$$\sigma=\sum_{k=0}^{N}\frac{(-1)^k}{(2k+1)}\frac{N!}{(N-k)!}\sum_{m=0}^{k}\frac{(-1)^m}{(k-m)!m!}\sigma\left[V(R)-\frac{N-3m}{2\sqrt{N(N+\frac{3}{2})}}f(R)\right], \tag{23}$$

where $\sigma(V(R))$ is the fusion cross section calculated using the one-dimensional barrier V(R).

Equation (23), calculated using the interacting boson model, resembles Eq. (1), calculated using the geometrical model, as expected. In the former, however, the number of included channels is determined by the boson number of the target nucleus, whereas one can include an arbitrary number of channels in the latter. Thus using IBM provides us a prescription to determine the number of channels to be included. When the boson number N is 1, the allowed values of angular momentum are $L=0$ and 2. In this case using IBM we get $\lambda_1=-0.316$, $\omega_1=0.667$ and $\lambda_2=0.633$, $\omega_2=0.333$ and using the geometrical model we get $\lambda_1=-0.327$, $\omega_1=0.652$ and $\lambda_2=0.613$, $\omega_2=0.348$. A comparison of these two models with three channels is given in Table I.

Except the two approximations described above [neglecting the excitation energies and the second term in Eq. (16)], Eq. (23) holds whatever method one uses to calculate the fusion cross section for the one-dimensional barrier. In particular, when the one-dimensional potential barrier has the same topological structure as a quadratic function, the penetration probability of Eq. (11a) can be calculated [20] in a uniform semiclassical approximation with a proper treatment of the multiple reflections under the barrier to obtain the usual WKB expression for penetrability:

$$P_0(E,V(R))=\left\{1+\exp\left[2\int_{r_1}^{r_2}\left[\frac{2\mu}{\hbar^2}[V(r)-E]\right]^{1/2}\right]\right\}^{-1}\ . \tag{24}$$

TABLE I. A comparison of the interacting boson model predictions for the weight factors and the channel eigenvalues in Eq. (1) with the geometrical model predictions for the case of three channels.

Model	ω_i	λ_i
IBM	0.533	−0.378
	0.267	0.190
	0.200	0.756
Geometrical model	0.468	−0.415
	0.361	0.156
	0.171	0.804

Equation (24) is valid uniformly from below to above the barrier. In this paper we will calculate the fusion cross section within this approximation. We take a Woods-Saxon form for the nuclear part of the potential

$$V_N(R)=-V_0/[1+\exp(R-R_0)/a]\ . \tag{25}$$

In Fig. 1 we exhibit the schematic behavior of the fusion cross section, Eq. (23), for different values of the boson number N. In this figure the cross section is plotted for the system of ^{16}O and ^{154}Sm. The dotted line is for $N=0$ (bare potential). The dashed line is for $N=1$ and the solid line is for $N=11$ (the actual boson number of ^{154}Sm). In calculating these cross sections we used the values $V_0=68$ MeV, $R_0=8.9$ fm, $a=0.95$ fm for the nuclear part of the heavy-ion interaction potential and $\beta_2=0.35$ for the deformation parameter for ^{154}Sm. This value of the deformation parameter β_2 is the one deduced from $B(E2)$ values by Raman *et al.* [21] In this figure

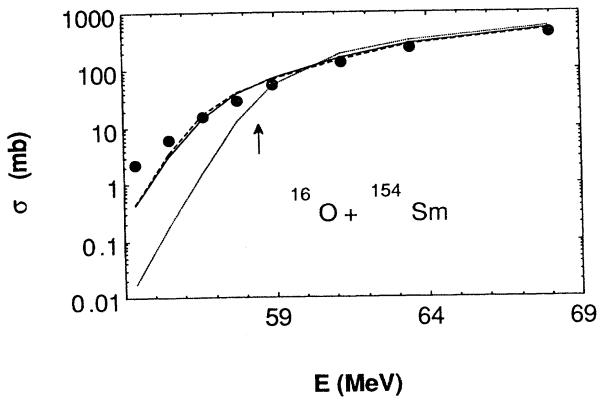

FIG. 1. The interacting boson model predictions of the fusion cross section for the system of ^{16}O and ^{154}Sm for different values of boson number, N. The dotted line is for $N=0$ (bare potential). The dashed line is for $N=1$ and the solid line is for $N=11$ (the actual boson number of ^{154}Sm). In calculating these cross sections Eq. (25) was used to describe the nuclear part of the heavy-ion interaction potential with the parameter values $V_0=68$ MeV, $R_0=8.9$ fm, $a=0.95$ fm, and $\beta_2\times R=0.35\times 6.43$ fm for ^{154}Sm. The data are from Ref. [22]. The arrow indicates the position of the barrier maximum.

the experimental data, indicated by black dots, are taken from Stokstad *et al.* [22] and the position of the barrier maximum energy of 58.2 MeV is indicated by an arrow. A salient feature of Fig. 1 is the quick convergence of the cross section as N (or the number of channels) increases. $N=1$ and the large values of N yield the same cross section. Since different symmetry chains of IBM give the same result for the transition probabilities when $N=1$, it would be desirable to find a quantity which depends on N in a more sensitive manner. One possibility is the average angular momentum

$$\langle L \rangle = \left[\sum_L L\sigma_L \right] / \sigma \ , \tag{26}$$

which can be determined reasonably accurately from the gamma-ray multiplicities data [23,24]. In Fig. 2 we present the average angular momentum for the system ^{16}O and ^{154}Sm calculated with $N=0$ (the dotted line), with $N=1$ (the dashed line), and with $N=11$ (the solid line). The same potential parameters as in Fig. 1 are used. Once again one observes that the average angular momentum converges rather quickly. Our analysis confirms the results of Ref. [25], where it was shown that it is sufficient to include a small number of channels in the coupled-channel calculations to obtain the correct distribution of potential barriers. One generally expects, in a rather model-independent way, the coupled-channel calculations to converge rapidly as the basis size is increased. Vandenbosch and his collaborators recently determined mean angular momenta for this reaction by two different techniques. They either observed low-lying gamma transitions in the evaporation residues or detected the residues directly by exploiting an electrostatic detector [24]. The first method has been applied with higher sensitivity than previously and the second method enables measurements at a lower energy than is possible with gamma-ray tagging techniques. The mean L values they deduced from these recent measurements are substantially higher than their previous data [23] and display prominently the mean-spin barrier bump. We exhibit the data from Ref. [24] in Fig. 2. Also shown is a full coupled-channels calculation (the dash-dotted line), reported in Ref. [24], using the coupled-channels code CC DEF [26] including quadrupole and hexadecapole deformations and octupole vibrations. One observes that the full coupled-channels calculation is in better agreement with experiment, but, like our calculation, it still underestimates the $\langle L \rangle$ values near the maximum barrier energy, indicated by an arrow. The difference between the CC DEF result and our calculation is easier to understand. In addition to neglecting the excitation energies, assuming the exact SU(3) limit we neglected hexadecapole deformations. Similarly excluded in the simplest version of IBM are the octupole vibrations. To describe octupole collectivity in IBM necessitates the introduction of an $f(L=3)$ boson [15]. It is also interesting to note that the $N=1$ calculation seems to approximate the data better than the $N=11$ calculation. We should remind the reader that for $N=1$ only the excitation of the first 2^+ state is included in the channel coupling [cf. the discussion following Eq. (23)], whereas $N=11$ includes the entire ground-state band.

Recently the fusion excitation function [27] and the gamma-ray multiplicities for the ^{16}O+^{166}Er system were measured and the average angular momenta were deduced [28]. In Fig. 3 we compare our calculation for this cross section (the solid line) with the data of Ref. [27] (black dots). Again Eq. (25) was used to describe the nuclear interaction with $V_0=80$ MeV, $R_0=8.55$ fm, $a=1.15$ fm with the deformation parameter [21] $\beta_2=0.341$. Also plotted is the result of the full coupled-channels calculation CC DEF (the dash-dotted line), including quadrupole and hexadecapole deformations and octupole vibrations, reported in Ref. [28]. In Fig. 4, IBM predictions for the average angular momenta are com-

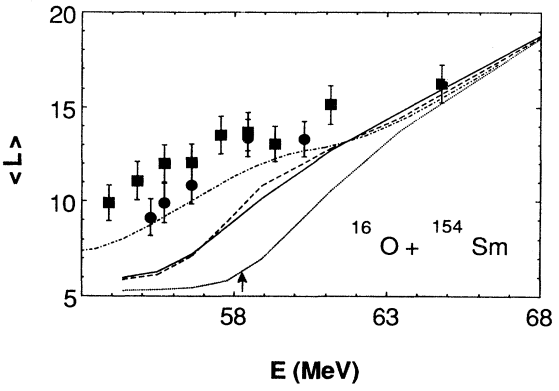

FIG. 2. The average angular momentum for the system ^{16}O and ^{154}Sm calculated with $N=0$ (the dotted line), with $N=1$ (the dashed line), and with $N=11$ (the solid line). The data are taken from Ref. [24] and the same potential parameters as in Fig. 1 are used. The circles represent data determined from Ge-tagged multiplicities and the squares those determined from the deflector-tagged multiplicities. The dot-dashed line is the full coupled-channels calculation reported in Ref. [24]. The arrow indicates the position of the barrier maximum.

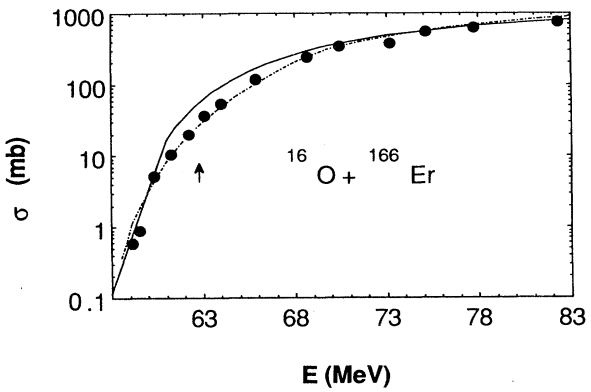

FIG. 3. Fusion cross section for the ^{16}O+^{166}Er system calculated as described in the text. The data (black dots) are from Ref. [27]. The solid line is the IBM prediction and the dot-dashed line is the full coupled-channels calculation reported in Ref. [28]. The arrow indicates the position of the barrier maximum.

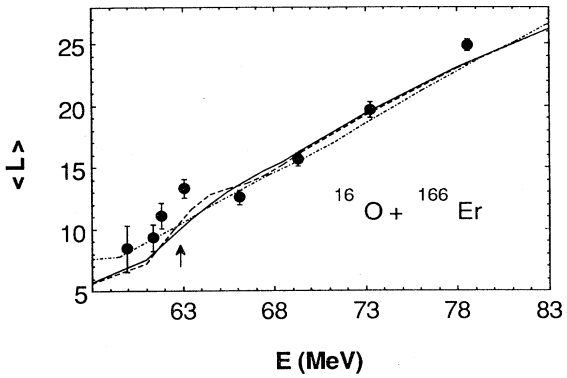

FIG. 4. IBM predictions (dashed line with $N=1$ and the solid line with $N=15$) for the average angular momenta for the $^{16}O+^{166}Er$ system calculated as described in the text. The data are from Ref. [28]. The dot-dashed line is the full coupled-channels calculation reported in Ref. [28]. The arrow indicates the position of the barrier maximum.

pared with the data of Ref. [28]. In this figure the dashed line is the calculation with $N=1$ and the solid line with $N=15$ (the actual boson number of ^{166}Er). The dash-dotted line is the full coupled-channel calculation mentioned above. One observes that our model predicts $\langle L \rangle$ reasonably well except for the barrier bump, where it underestimates the data. This failure seems to be a common feature of a large class of models [24]. Indeed when the coupling gets stronger the barrier bump gets stronger. To demonstrate this behavior in Fig. 5 we present the average angular momentum for three different values of $\beta_2 R$: 0 (the dashed line), 0.1286 fm (the dotted line), and 0.2572 fm (the solid line). Figure 4, like Fig. 2, also reveals that the $N=1$ calculation is actually a better approximation to the mean angular momentum bump than $N=15$ calculation; averaging over many channels seem to smear the mean-spin bump. A very pronounced broadening of the $\langle L \rangle$ distribution can thus be a signature of exciting only few low-lying states as well as the increased strength of the coupling.

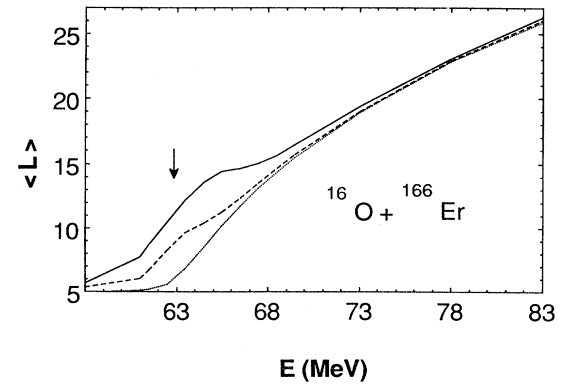

FIG. 5. Average angular momentum calculated using the IBM based model (with $N=1$) for the $^{16}O+^{166}Er$ system using $\beta_2 R$: 0 (the dotted line), 0.1286 fm (the dashed line), and 0.2572 fm (the solid line).

IV. SUMMARY

We have discussed the inclusion of nuclear structure effects in fusion reactions below the Coulomb barrier using the interacting boson model and given simple approximate expressions for the fusion cross section and the mean angular momentum. We employed the simplest version of IBM, the so-called IBM-1 ignoring the mixed-symmetry states and octupole collectivity. Mixed symmetry states [29,30] are unimportant in low-energy fusion since they have relatively high excitation energies (~ 3 MeV). In contrast, the octupole and higher multipole vibrations contribute significantly to sub-barrier fusion as we demonstrated in Sec. III. Although we only focused on the fusion of axially symmetric [i.e., SU(3)] nuclei in this paper, our technique can easily be applied to the vibrational [SU(5)] or gamma-unstable [SO(6)] nuclei, as we shall present in future publications.

Following the algebraic treatment in Ref. [12] of medium-energy proton-nucleus scattering, Amado and collaborators formulated the inelastic scattering of electrons off molecules [31] algebraically using the vibron model [32]. An application of the techniques developed in our paper to inelastic nuclear scattering was given in Ref. [16]. It is similarly possible to utilize the formalism of Amado and his collaborators within the path integral description developed in this paper to describe inelastic molecule-molecule scattering, as will be reported elsewhere.

ACKNOWLEDGMENTS

This research was supported in part by the University of Wisconsin Research Committee with funds granted by the Wisconsin Alumni Research Foundation, and in part by the U.S. National Science Foundation Grant No. PHY-9015255. The research of A.B.B. was further supported in part by the Presidential Young Investigator Program administered by the U.S. National Science Foundation.

APPENDIX: "ROTATING-FRAME" APPROXIMATION IN THE INFLUENCE FUNCTIONAL

In this appendix we wish to elucidate the physical meaning of the approximation done in the text following Eq. (16). The time derivative in the second term of this equation can easily be evaluated resulting in an expression of the form

$$i\hbar\frac{\partial U^{(0)}}{\partial t}=\left[H^{(0)}(R(t))-i\hbar\sum_{\mu=-1}^{1}\alpha_\mu\left[\frac{d\hat{\mathbf{R}}(t)}{dt}\right]L_\mu\right]U^{(0)}, \tag{A1}$$

where L_μ are the angular momentum operators. The dependence of the functions α_μ on $d\hat{\mathbf{R}}(t)/dt$ can be calculated as well, but for the following argument it is sufficient to note that the former goes to zero as the latter vanishes. Let us assume that initially we are in the ground state of the target nucleus with angular momentum $L=0$. The state of the nucleus after time T is given by

$$U(\mathbf{R}(t))|0\rangle=\mathcal{R}(\hat{\mathbf{R}}(t))U^{(0)}(\mathbf{R}(t))|0\rangle . \tag{A2}$$

Solving Eq. (A1) in first-order perturbation theory we find this state to be

$$\mathcal{R}(\hat{\mathbf{R}}(t))[\exp(-iH^{(0)}T/\hbar)]\times\left[1+\frac{i}{\hbar}\int_0^T dt[\exp(iH^{(0)}T/\hbar)]\sum\alpha_\mu L_\mu\right]|0\rangle . \tag{A3}$$

One observes that the first term which contains the term $\exp(-iH^{(0)}T/\hbar)$, where $H^{(0)}$ is given by Eq. (13b), excites solely the $M=0$ substates due to the tensorial structure of $H^{(0)}$, whereas the second term would excite those substates with $M\neq 0$. Upon substituting Eq. (A3) into the influence functional, Eq. (12), the term $\mathcal{R}(\hat{\mathbf{R}}(t))$ drops out due to unitarity. Consequently, if α_μ [or equivalently $d\hat{\mathbf{R}}(t)/dt$] vanish, only the $M=0$ magnetic substates contribute to the influence functional as in the rotating-frame approximation of Ref. [16].

[1] M. Beckerman, Rep. Prog. Phys. **51**, 1047 (1988).
[2] H. Esbensen, Nucl. Phys. **A352**, 147 (1981).
[3] D. M. Brink, M. C. Nemes, and D. Vautherin, Ann. Phys. (N.Y.) **147**, 171 (1983).
[4] C. H. Dasso, S. Landowne, and A. Winther, Nucl Phys. **A405**, 381 (1983); **A432**, 555 (1985).
[5] H. J. Krappe, K. Mohring, M. C. Nemes, and H. Rossner, Z. Phys. A **314**, 23 (1983).
[6] A. B. Balantekin and N. Takigawa, Ann. Phys. (N.Y.) **160**, 441 (1985).
[7] D. M. Chase, L. Wilets, and A. R. Edmonds, Phys. Rev. **110**, 1080 (1958).
[8] M. A. Nagarajan, A. B. Balantekin, and N. Takigawa, Phys. Rev. C **34**, 894 (1986).
[9] R. Lindsay and N. Rowley, J. Phys. G **10**, 805 (1984).
[10] A. Bohr and B. Mottelson, Dan. Vid. Selskab. Mat. Fys. Medd. **27**, 16 (1953).
[11] A. Arima and F. Iachello, in *Advances in Nuclear Physics,* edited by J. W. Negele and E. Vogt (Plenum, New York, 1984), Vol. 13, pp. 139–198.
[12] J. N. Ginocchio, T. Otsuka, R. D. Amado, and D. A. Sparrow, Phys. Rev. C **33**, 247 (1986).
[13] J. N. Ginocchio, Nucl. Phys. **A421**, 369c (1984).
[14] N. Takigawa and K. Ikeda, in *Proceedings of the Symposium on Many Facets of Heavy Ion Fusion Reactions,* edited by W. Henning *et al.* (Argonne National Laboratory Report ANL-PHY-86-1, 1986), pp. 613–620.
[15] O. Tanimura, Phys. Rev. C **35**, 1600 (1987).
[16] H. Esbensen, S. Landowne, and C. Price, Phys. Rev. C **36**, 1216 (1987); **36**, 2359 (1987).
[17] N. Takigawa, F. Michel, A. B. Balantekin, and G. Reidemeister, Phys. Rev C **44**, 477 (1991).
[18] A. Arima and F. Iachello, Ann. Phys. (N.Y.) **111**, 201 (1978).
[19] J. N. Ginocchio and M. W. Kirson, Nucl. Phys. **A350**, 31 (1980); A. E. L. Dieperink, O. Scholten, and F. Iachello, Phys. Rev. Lett. **44**, 1747 (1980).
[20] D. M. Brink and U. Smilansky, Nucl. Phys. **A405**, 301 (1983).
[21] S. Raman *et al.*, At. Data Nucl. Data Tables **36**, 1 (1987).
[22] R. G. Stokstad *et al.*, Phys. Rev. C **21**, 2427 (1980).
[23] R. Vandenbosch *et al.*, Phys. Rev. C **28**, 1161 (1983); S. Gil *et al.*, *ibid.* **31**, 1752 (1985).
[24] S. Gil *et al.*, Phys. Rev. C **43**, 701 (1991).
[25] N. Rowley, G. R. Satchler, and P. H. Stelson, Phys. Lett. B **254**, 25 (1991).
[26] J. Fernandez Niello, C. H. Dasso, and S. Landowne, Comput. Phys. Commun. **54**, 409 (1989).
[27] J. O. Fernandez Niello *et al.*, Phys. Rev. C **43**, 2303 (1991).
[28] S. Gil *et al.*, Phys. Rev. Lett. **65**, 3100 (1990).
[29] D. Bohle *et al.*, Phys. Lett. **137B**, 27 (1984).
[30] A. B. Balantekin and B. R. Barrett, Phys. Rev. C **32**, 288 (1985).
[31] R. Bijker, R. D. Amado, and D. A. Sparrow, Phys. Rev. A **33**, 871 (1986); R. Bijker and R. D. Amado, *ibid.* **34**, 71 (1986); **37**, 1425 (1988).
[32] F. Iachello, Chem. Phys. Lett. **78**, 581 (1981); F. Iachello and R. D. Levine, J. Chem. Phys. **77**, 3046 (1982).